

Kinetic Studies on the Cobalt-Catalyzed Norbornadiene Intermolecular Pauson–Khand Reaction

Rafel Cabot, Agustí Lledó, Marc Revés, Antoni Riera,* and Xavier Verdager*

Unitat de Recerca en Síntesi Asimètrica (URSA-PCB), Institute for Research in Biomedicine (IRB), and Departament de Química Orgànica, Universitat de Barcelona, c/Josep Samitier, 1-5, E-08028 Barcelona, Spain

Received October 11, 2006

The kinetics for the cobalt-catalyzed intermolecular Pauson–Khand reaction (PKR) between (trimethylsilyl)acetylene and norbornadiene (NBD) at a constant CO pressure has been studied by means of in situ FT-IR. The rate dependence on catalyst and substrate concentrations was examined, and it was found that the process is -1.9 order with respect to CO pressure, zero order with respect to acetylene, 0.3 – 1.2 order with respect to NBD, and 1.3 order with respect to the $\text{Co}_2(\text{CO})_8$ catalyst. Catalytic reaction intermediates were examined by their corresponding metal carbonyl IR frequencies. By a one-pot consecutive Pauson–Khand experiment, the NBD–dicobalt hexacarbonyl complex was identified as a catalytically active complex. $\text{Co}_4(\text{CO})_{12}$ was also studied as a catalyst source in the PKR. Analysis of the corresponding reaction intermediates by IR demonstrated that $\text{Co}_2(\text{CO})_8$ and $\text{Co}_4(\text{CO})_{12}$ provide identical intermediate profiles upon reaction with TMSC_2H . The experimental measured kinetics are consistent with the alkene insertion being the rate-limiting step in the catalytic PKR. Finally, the effect of phosphine substitution on the catalyst and the use of Lewis acid additives were shown to have a deleterious effect on the reaction rate.

Introduction

Since its discovery in the 1970s, the Pauson–Khand reaction (PKR) has attracted major interest from the community of chemists¹ because it provides the most straightforward access to cyclopentenone compounds, which in turn are valuable synthetic intermediates in natural product synthesis.^{2,3} The reaction was first described to be either promoted or catalyzed by $\text{Co}_2(\text{CO})_8$. Enormous research effort has since been devoted to exploring other metal sources to effect this transformation.⁴ Despite this effort, dicobalt octacarbonyl has remained the most simple and convenient choice to run the reaction.

At present, even when only $\text{Co}_2(\text{CO})_8$ is used as a metal source, a myriad of reaction conditions have been developed to improve the reaction yields and broaden the substrate scope. The use of Lewis bases as additives in the stoichiometric and

catalytic PKR is well documented. Thus, soft and hard Lewis bases, such as phosphine oxides,⁵ sulfides,⁶ sulfoxides,⁷ thioureas,⁸ amines,⁹ and water,¹⁰ have been described to enhance the catalytic PKR. The pressure of CO used in the catalytic PKR is also a subject of debate. Initially, efficient catalytic reactions were described at high temperature and CO pressure (10–40 atm).¹¹ Later, a PKR at atmospheric CO pressure using $\text{Co}_2(\text{CO})_8$ as catalyst was described.¹² Several studies argue the convenience of using high-intensity visible light as a promoter

* To whom correspondence should be addressed. E-mail: xverdager@pcb.ub.es (X.V.).

(1) (a) Khand, I. U.; Knox, G. R.; Pauson, P. L.; Watts, W. E.; Foreman, M. I. *J. Chem. Soc., Perkin Trans. 1* **1973**, 977–981. (b) Khand, I. U.; Knox, G. R.; Pauson, P. L.; Watts, W. E. *J. Chem. Soc., Chem. Commun.* **1971**, 36.

(2) For selected reviews in the field see: (a) Brummond, K. M.; Kent, J. L. *Tetrahedron* **2000**, *56*, 3263–3283. (b) Buchwald, S. L.; Hicks, F. A. In *Comprehensive Asymmetric Catalysis I-III*; Springer-Verlag: Berlin, 1999; pp 491–510. (c) Geis, O.; Schmalz, H.-G. *Angew. Chem., Int. Ed.* **1998**, *37*, 911–914. (d) Gibson, S. E.; Stevenazzi, A. *Angew. Chem., Int. Ed.* **2003**, *42*, 1800–1810. (e) Ingate, S. T.; Marco-Contelles, J. *Org. Prep. Proced. Int.* **1998**, *30*, 121–143. (f) Schore, N. E. *Org. React.* **1991**, *40*, 1–90. (g) Sugihara, T.; Yamaguchi, M.; Nishizawa, M. *Chem. Eur. J.* **2001**, *7*, 1589–1595. (h) Gibson, S. E.; Mainolfi, N. *Angew. Chem., Int. Ed.* **2005**, *44*, 3022–3037. (i) Laschat, S.; Becheanu, A.; Bell, T.; Baro, A. *Synlett* **2005**, 2547–2570.

(3) For recent examples of Pauson–Khand applications in total synthesis see: (a) Caldwell, J. J.; Cameron, I. D.; Christie, S. D. R.; Hay, A. M.; Johnstone, C.; Kerr, W. J.; Murray, A. *Synthesis* **2005**, 3293–3296. (b) Ishizaki, M.; Niimi, Y.; Hoshino, O.; Hara, H.; Takahashi, T. *Tetrahedron* **2005**, *61*, 4053–4065. (c) Tang, Y.; Zhang, Y.; Dai, M.; Luo, T.; Deng, L.; Chen, J.; Yang, Z. *Org. Lett.* **2005**, *7*, 885–888. (d) Winkler, J. D.; Lee, E. C. Y.; Nevels, L. I. *Org. Lett.* **2005**, *7*, 1489–1491.

(4) Titanium: (a) Hicks, F. A.; Kablaoui, N. M.; Buchwald, S. L. *J. Am. Chem. Soc.* **1999**, *121*, 5881–5898. (b) Hicks, F. A.; Buchwald, S. L. *J. Am. Chem. Soc.* **1999**, *121*, 7026–7033. Molybdenum: (c) Jeong, N.; Lee, S. J.; Lee, B. Y.; Chung, Y. K. *Tetrahedron Lett.* **1993**, *34*, 4027–4030. (d) Adrio, J.; Rivero, M. R.; Carretero, J. C. *Org. Lett.* **2005**, *7*, 431–434. (e) Brummond, K. M.; Kerekes, A. D.; Wan, H. *J. Org. Chem.* **2002**, *67*, 5156–5163. Ruthenium: (f) Kondo, T.; Suzuki, N.; Okada, T.; Mitsudo, T. *J. Am. Chem. Soc.* **1997**, *119*, 6187–6188. (g) Morimoto, T.; Fujii, K.; Tsutsumi, K.; Kakiuchi, K. *J. Am. Chem. Soc.* **2002**, *124*, 3806–3807. Iridium: (h) Shibata, T.; Takagi, K. *J. Am. Chem. Soc.* **2000**, *122*, 9852–9853. Rhodium: (i) Jeong, N. *Organometallics* **1998**, *17*, 3642–3644. (j) Jeong, N.; Sung, B. K.; Choi, Y. K. *J. Am. Chem. Soc.* **2000**, *122*, 6771–6772. (k) Mukai, C.; Inagaki, F.; Yoshida, T.; Yoshitani, K.; Hara, Y.; Kitagaki, S. *J. Org. Chem.* **2005**, *70*, 7159–7171.

(5) Billington, D. C.; Helps, I. M.; Pauson, P. L.; Thomson, W.; Willison, D. *J. Organomet. Chem.* **1988**, *354*, 233–242.

(6) Sugihara, T.; Yamada, M.; Yamaguchi, M.; Nishizawa, M. *Synlett* **1999**, 771–773.

(7) Chung, Y. K.; Lee, B. Y.; Jeong, N.; Hudecek, M.; Pauson, P. L. *Organometallics* **1993**, *12*, 220–223.

(8) Tang, Y.; Deng, L.; Zhang, Y.; Dong, G.; Chen, J.; Yang, Z. *Org. Lett.* **2005**, *7*, 593–595.

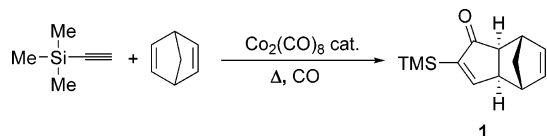
(9) Sugihara, T.; Yamada, M.; Ban, H.; Yamaguchi, M.; Kaneko, C. *Angew. Chem., Int. Ed.* **1998**, *36*, 2801–2804.

(10) (a) Sugihara, T.; Yamaguchi, M. *Synlett* **1998**, 1384–1386. (b) Sugihara, T.; Yamaguchi, M.; Nishizawa, M. *Chem. Eur. J.* **2001**, *7*, 1589–1595.

(11) Rautenstrauch, V.; Megard, P.; Conesa, J.; Kuester, W. *Angew. Chem., Int. Ed. Engl.* **1990**, *29*, 1413–1416.

(12) (a) Pagenkopf, B. L.; Livinghouse, T. *J. Am. Chem. Soc.* **1996**, *118*, 2285–2286. (b) Belanger, D. B.; O'Mahony, D. J. R.; Livinghouse, T. *Tetrahedron Lett.* **1998**, *39*, 7637–7640.

Scheme 1 . Catalytic Intermolecular PKR Used in the Present Study



or extra-pure $\text{Co}_2(\text{CO})_8$ in thermally activated processes. Recently, commercial grade $\text{Co}_2(\text{CO})_8$ has been shown to be active in the catalytic PKR at atmospheric CO pressure in the presence of cyclohexylamine.¹³

In contrast to other metal-catalyzed processes, a general catalytic asymmetric version of the PKR has remained elusive. Recent developments in this field have focused on intramolecular reactions, many of which are mediated by metals other than cobalt.^{4b,h,j} Bis(phosphine) and bis(phosphite) dicobalt carbonyl complexes have been successfully applied to the intramolecular catalytic PKR.¹⁴ However, although in some instances high enantiomeric excess is achieved, the catalytic systems are not very active with respect to turnover frequencies (TOF).

Our research group has a longstanding interest in the development of enantioselective versions of the PKR. We have developed several chiral auxiliary based asymmetric PKRs.¹⁵ More recently, we examined the use of chiral bidentate (P,S) ligands in the stoichiometric intermolecular PKR.¹⁶ This led to the effective synthesis of optically pure (+)-*exo*-4-(trimethylsilyl)tricyclo[5.2.1.0^{2,6}]-4,8-decadien-3-one (**1**). In turn, this product has been shown to be a valuable synthon in the synthesis of phytoprostanes and, thus, we focused our attention on the large-scale preparation of **1** in racemic form.¹⁷ For this purpose, we examined the cobalt-catalyzed preparation of **1** (Scheme 1). To our knowledge, there are no reliable kinetic data on the catalytic PKR. Here we report a complete kinetic study of $\text{Co}_2(\text{CO})_8$ -catalyzed intermolecular PKR between (trimethylsilyl)ethyne and norbornadiene by means of in situ FT-IR techniques.

Results and Discussion

Kinetic measurements were conducted under constant CO pressure in a 50 mL medium-pressure glass reactor mounted with a stainless steel cap and fitted with an immersible in situ FT-IR SiComp probe. The CO pressure was controlled and maintained constant in the reaction vessel by means of a low-pressure manometer. To obtain data for the representative reaction conditions in the synthesis of **1** and to avoid catalyst decomposition, the working CO overpressure¹⁸ was fixed between 1 and 4.0 bar; however, most reactions were performed

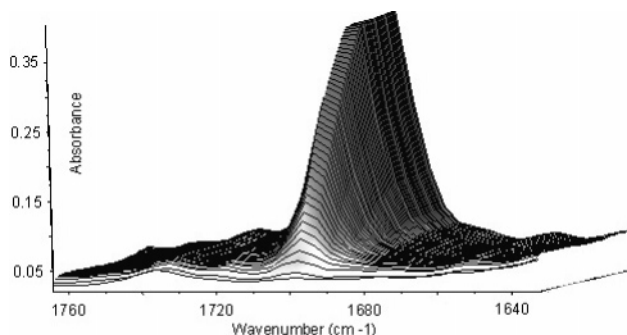


Figure 1. Representative three-dimensional stack plot of IR spectra collected every 5 min for the catalytic PKR between TMS- C_2H and NBD.

at 2 bar. Toluene was the solvent of choice because of its high boiling point. (Trimethylsilyl)ethyne (TMS- C_2H) was the limiting substrate when not stated otherwise. The excess of norbornadiene (NBD) was fixed at 2.0 equiv for most experiments. Under the standard reaction conditions (77 °C, 2 bar of CO, $[\text{Co}_2(\text{CO})_8] = 12.7 \text{ mM}$), a variation of stirring speed between 100 and 1100 rpm did not affect the initial reaction rates. This excludes CO mass transport interferences in the resulting kinetic data.¹⁹ The purity of dicobalt octacarbonyl catalyst was a major concern, since it could greatly affect the kinetic measurements. To check this, commercial $\text{Co}_2(\text{CO})_8$ stabilized with hexanes (10 wt %) was compared with a sublimed catalyst sample. Reaction rates obtained using the purified catalyst were identical with those of the commercial sample. Therefore, commercial $\text{Co}_2(\text{CO})_8$ without further purification was used in the study.²⁰ In all cases reactions remained homogeneous throughout the kinetic experiments.

Reaction progress analysis was performed by monitoring the characteristic carbonyl (C=O) stretching absorbance of product **1** at 1698 cm^{-1} . The carbonyl stretching of **1** was undisturbed by other IR absorbances in the reaction mixture (Figure 1). From all spectra collected every 5 min, an absorbance vs time profile was constructed, which graphically reflects the reaction progress (Figure 2). Gas chromatography (GC) analysis of the resulting final reaction mixture showed that the tricyclopentenone **1** was the major product (90%); however, the corresponding diketones **2a** (5.2%) and **2b** (4.8%) resulting from double PKR onto NBD were also present (Figure 3).^{1a} Assessment of the reaction progress by GC analysis allowed us to determine that depletion of the limiting substrate (alkyne) from the reaction mixture brings the production of **1** to an end (Figure 2). GC analysis confirmed that formation of **2a** and **2b** is a negligible side reaction within the first 2 h of the catalytic PKR, and therefore, it should not disturb initial reaction rate measurements. The absorbance profile for the buildup of **1** showed that there is no induction period in the PKR studied here.

The PKRs of norbornadiene (NBD) and norbornene are known to be highly stereoselective, affording almost exclusively exo cycloadducts, such as the one depicted in Scheme 1.^{1a} Analysis of the final reaction mixtures by HPLC revealed that variable amounts of the corresponding endo cyclopentenone as a minor product could be observed, depending on the reaction

(13) Krafft, M. E.; Boñaga, L. V. R.; Hirotsawa, C. *J. Org. Chem.* **2001**, *66*, 3004–3020.

(14) (a) Hiroi, K.; Watanabe, T.; Kawagishi, R.; Abe, I. *Tetrahedron Lett.* **2000**, *41*, 891–895. (b) Gibson, S. E.; Kaufmann, K. A. C.; Loch, J. A.; Steed, J. W.; White, A. J. P. *Chem. Eur. J.* **2005**, *11*, 2566–2576.

(15) (a) Verdaguier, X.; Moyano, A.; Pericàs, M. A.; Riera, A.; Bernardes, V.; Greene, A. E.; Alvarez-Larena, A.; Piniella, J. F. *J. Am. Chem. Soc.* **1994**, *116*, 2153–2154. (b) Marchueta, I.; Montenegro, E.; Panov, D.; Poch, M.; Verdaguier, X.; Moyano, A.; Pericàs, M. A.; Riera, A. *J. Org. Chem.* **2001**, *66*, 6400–6409.

(16) (a) Solà, J.; Riera, A.; Verdaguier, X.; Maestro, M. A. *J. Am. Chem. Soc.* **2005**, *127*, 13629–13633. (b) Verdaguier, X.; Moyano, A.; Pericàs, M. A.; Riera, A.; Maestro, M. A.; Mahia, J. J. *J. Am. Chem. Soc.* **2000**, *122*, 10242–10243. (c) Verdaguier, X.; Lledó, A.; Lopez-Mosquera, C.; Maestro, M. A.; Pericàs, M. A.; Riera, A. *J. Org. Chem.* **2004**, *69*, 8053–8061.

(17) Iqbal, M.; Evans, P.; Lledó, A.; Verdaguier, X.; Pericàs, M. A.; Riera, A.; Loeffler, C.; Sinha, A. K.; Mueller, M. J. *ChemBioChem* **2005**, *6*, 276–280.

(18) Unless stated otherwise, throughout the present study the working CO pressure will be expressed in bar above atmospheric pressure.

(19) The stirring speed was set to 1100 rpm for all of the kinetic measurements. A cross-shaped magnetic stirrer was used throughout the present study. For the effect of stirring speed on asymmetric hydrogenations see: Sun, Y.; Landau, R. N.; Wang, J.; LeBlond, C.; Blackmond, D. G. *J. Am. Chem. Soc.* **1996**, *118*, 1348–1353.

(20) Sublimed $\text{Co}_2(\text{CO})_8$ samples are far more sensitive to moisture and oxygen than the corresponding commercial hexanes-stabilized samples.

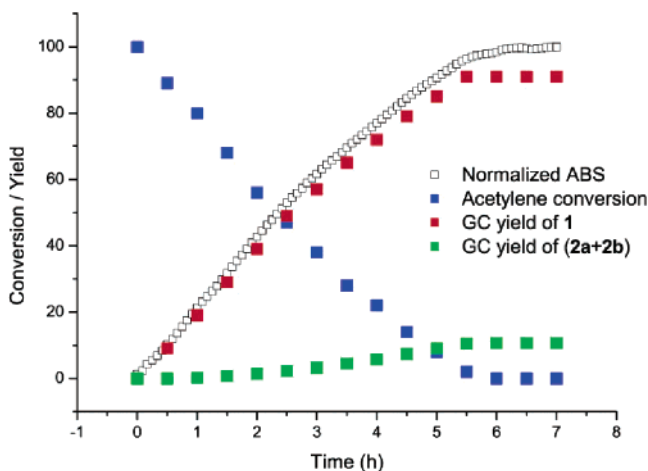


Figure 2. Reaction profile of the IR spectra collected every 5 min for the catalytic PKR (black squares). Conditions: $[\text{TMSC}_2\text{H}]_0 = 0.41 \text{ M}$, $[\text{NBD}]_0 = 0.84 \text{ M}$, CO pressure 2 bar, 77°C , $[\text{Co}_2(\text{CO})_8] = 14.3 \text{ mM}$, 2 bar of CO, 77°C . In addition, product formation and acetylene depletion as determined by GC analysis are shown.

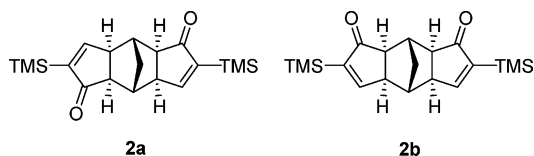


Figure 3. Compounds resulting from double cyclization on NBD detected in the catalytic intermolecular PKR.

conditions (vide infra). In the present study, both stereoisomers were considered as a whole the product of the reaction.

The first issue we addressed was whether the present catalytic system undergoes catalyst deactivation. To verify this, we used reaction progress kinetic analysis tools. Blackmond and co-workers showed that representation of the instantaneous reaction rates vs the limiting substrate concentration is an excellent method to determine whether a catalytic system undergoes catalyst deactivation or product inhibition.²¹ Thus, we proceeded to measure the reaction profile at two initial alkyne concentrations, $[\text{TMSC}_2\text{H}]_0 = 0.42, 0.30 \text{ M}$, with the same excess of NBD, $[\text{NBD}_{\text{excess}}] = 0.42 \text{ M}$. A graphical representation of the reaction rate vs the alkyne concentration for these two experiments provides two straight lines superimposed on each other (see Figure 1-S in the Supporting Information).²² This observation implies that under the present experimental conditions catalyst deactivation and product inhibition can be ruled out. Thus, we can assert that $\text{Co}_2(\text{CO})_8$ alone is a convenient catalyst source for the catalytic intermolecular PKR.

Reaction order with respect to catalyst concentration was studied with four catalyst loadings: i.e., 1, 2, 3, and 4 mol % at 77°C and 2 bar of CO. The corresponding reaction profiles are shown graphically in Figure 4. The $\text{Co}_2(\text{CO})_8$ concentration greatly affected reaction rates. While the reaction at 4 mol % of catalyst loading took 5 h to reach completion (black curve), the reaction took around 15 h (red curve) when the loadings were reduced to half (2 mol %). To find the corresponding reaction order with respect to $\text{Co}_2(\text{CO})_8$, a log/log plot of the initial reaction rates vs the catalyst concentration was constructed.²³ Linear fitting of data provided a slope of 1.35 with an *R* factor of 0.99 (Figure 4).

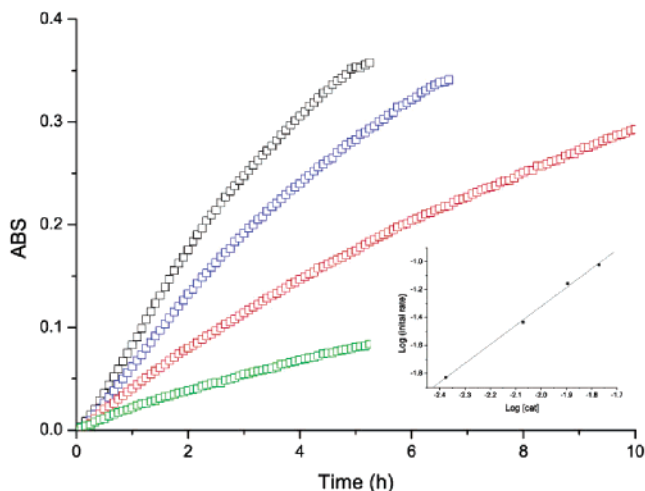


Figure 4. Reaction profile dependence on catalyst loading. Conditions: $[\text{TMSC}_2\text{H}]_0 = 0.42 \text{ M}$, $[\text{NBD}]_0 = 0.84 \text{ M}$, CO pressure 2 bar, 77°C . $[\text{Co}_2(\text{CO})_8]$: (black curve) 16.9 mM; (blue curve) 12.7 mM; (red curve) 8.5 mM; (green curve) 4.2 mM. Inset: plot of \log (initial rate) vs \log $[\text{Co}_2(\text{CO})_8]$, providing a slope of 1.35.

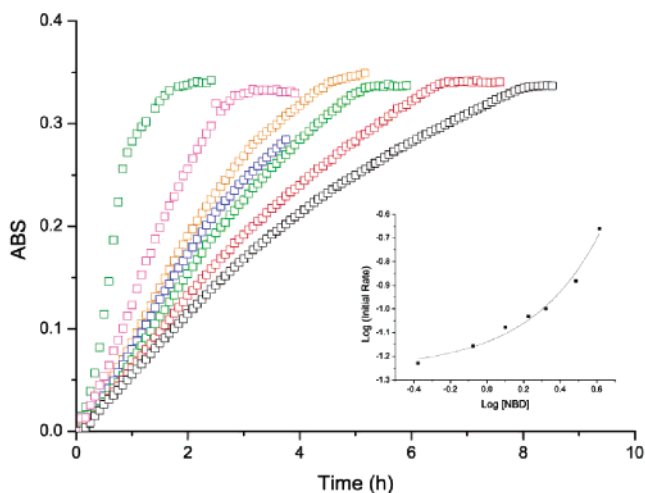


Figure 5. Reaction profile dependence on NBD concentration. Conditions: $[\text{TMSC}_2\text{H}]_0 = 0.42 \text{ M}$, $[\text{Co}_2(\text{CO})_8] = 12.7 \text{ mM}$, CO pressure 2 bar, 77°C . $[\text{NBD}]_0$: (black curve) 0.42 M; (red curve) 0.84 M; (green curve) 1.26 M; (blue curve) 1.68 M; (orange curve) 2.10 M; (pink curve) 3.07 M; (dark green curve) 4.20 M. Inset: plot of \log (initial rate) vs \log $[\text{NBD}]$.

The effect of acetylene concentration on the present catalytic system was studied further. As shown in Figure 2, when an excess of NBD was used, the reaction profile was suddenly truncated when TMSC_2H , the limiting substrate, was depleted from the reaction media. In addition, four reactions with identical $[\text{NBD}]_0$ (0.42 M) and distinct $[\text{TMSC}_2\text{H}]_0$ (0.30, 0.42, 0.60, and 0.79 M) were monitored and afforded identical initial rate profiles (see Figure 2-S in the Supporting Information). This behavior is indicative of zero-order (saturation) kinetics with respect to acetylene concentration.

To check the contribution of alkene concentration, a series of reactions were made at distinct $[\text{NBD}]_0$ while maintaining the rest of the parameters constant. The reactions were performed using a range of NBD between 1 and 10 equiv (0.42–4.20 M) with respect to TMSC_2H . To find the order dependence with respect to $[\text{NBD}]$, a log/log plot of the initial reaction rates vs the alkene concentration was constructed (Figure 5). From a qualitative point of view, olefin concentration had a positive effect on the reaction rate of the catalytic PKR. The reaction

(21) Blackmond, D. G. *Angew. Chem., Int. Ed.* **2005**, *44*, 4302–4320.

(22) The rate was obtained from fitting concentration–time data to an exponential curve and differentiating this function to obtain rate–time data.

(23) Birk, J. P. *J. Chem. Educ.* **1976**, *53*, 704–707.

Table 1. Exo to Endo Ratio of **1** and Percentage of **2a** + **2b** for the Catalytic PKR at Several NBD Concentrations

[NBD] ₀ (M (equiv))	exo:endo ^a	2a + 2b (%) ^{a,b}
0.42 (1)	22:1	14.3
1.26 (3)	17:1	2.8
1.68 (4)	14:1	2.1
4.20 (10)	10:1	0.8

^a Determined by HPLC analysis of the final reaction mixture. ^b Percentage of areas of **2a** and **2b** with respect to total **1**. No correction based upon extinction coefficient has been applied.

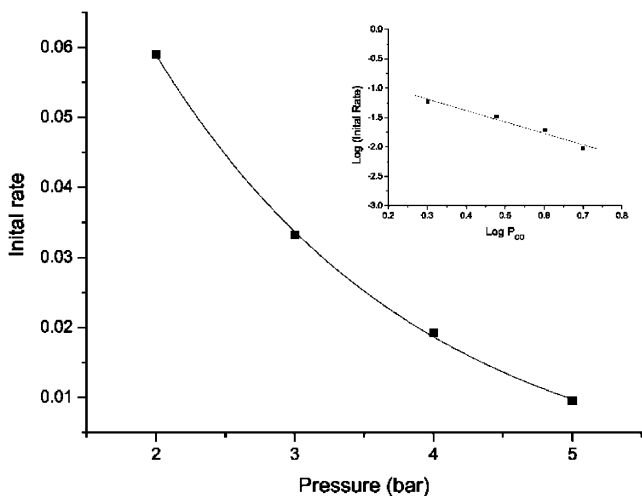


Figure 6. Initial rates vs absolute CO pressure. Reaction conditions: 70 °C, [Co₂(CO)₈] = 11.9 mM, [TMSC₂H]₀ = 0.41 M, [NBD]₀ = 0.82 M. Inset: plot of log (initial rate) vs log P_{CO}, providing a slope of -1.93.

order with respect to NBD was not constant in the range of NBD concentrations assayed and increased for high olefin concentrations. Curve fitting of data shown in Figure 5 and differentiation provided reaction orders between 0.3 and 1.2.²³ Analysis of the reaction mixtures revealed that NBD concentration had an effect on the stereoselectivity of the PKR (Table 1). Thus, the ratio of endo adduct increased as the concentrations of the alkene were augmented, while the amount of subproducts **2a** and **2b** in the final reaction mixture decreased.

We also performed a series of experiments to determine the dependence of the intermolecular PKR with respect to CO pressure. There has been much discussion about the need to run the reaction under either high or low pressures of CO;^{12,13} however, to date, no kinetic data on this issue have been reported. To address this question, four experiments were performed at CO pressures between 1 and 4 bar and at 70 °C. CO shows low solubility in organic nonpolar solvents. Under our experimental conditions, the CO concentration ranged between 8 and 40 mM.²⁴ Initial reaction rates were measured and plotted against absolute CO pressure (Figure 6). A negative order dependence of the reaction rate with respect to CO pressure was observed. A log/log plot of the initial reaction rates vs the absolute CO pressure afforded a -1.93 (*R* = 0.98) order dependence with respect to CO pressure (Figure 6). The influence of the CO pressure on the stereoselectivity of the cyclization was also examined and was found to be critical (Table 2). Low CO pressure maximizes the formation of the minor endo adduct, while higher pressures afforded increased exo selectivities.

(24) (a) Lühring, P.; Schumpe, A. *J. Chem. Eng. Data* **1989**, *34*, 250–252. (b) Jáuregui-Haza, U. J.; Pardillo-Fontdevila, E. J.; Wilhelm, A. M.; Delmas, H. *Latin Am. Appl. Res.* **2004**, *34*, 71–74.

Table 2. Exo to Endo Ratio of **1** and Percentage of **2a** + **2b** for the Catalytic PKR at Several CO Pressures

abs CO press (bar)	exo:endo ^a	2a + 2b (%) ^{a,b}
2	6:1	3.2
3	19:1	
4	34:1	6.2

^a Determined by HPLC analysis of the final reaction mixture. ^b Percentage of areas of **2a** and **2b** with respect to total **1**. No correction based upon extinction coefficient has been applied.

Catalytic Intermediates in the PKR. Analysis of the metal carbonyl area during the PKR may provide valuable information on the catalytic species in the reaction media. Here we set up the reactions by adding the catalyst, Co₂(CO)₈ (2069, 2042, 2023, 1849 cm⁻¹ in toluene), to a mixture of TMSC₂H and NBD. From initial moments, three major absorbances were detected at 2092, 2050, and 2023 cm⁻¹ (Figure 7), which correspond to the stretching of terminal COs in the Co₂(CO)₆-TMSC₂H complex **3** (Figure 8). It is well-known that the first step in the stoichiometric PKR is the formation of the alkyne dicobalt complex.^{1a} These absorbances were the only visible signals in the metal carbonyl region throughout the reaction. However, when the limiting substrate was depleted, another metal carbonyl compound emerged with absorbances at 2069, 2019 (broad), and 1826 cm⁻¹ (Figure 7).²⁵ The absorbance observed at 1826 cm⁻¹ is indicative of bridging carbonyl ligands but does not correspond to the initial Co₂(CO)₈, as could be expected. Instead, it corresponded to the dicobalt hexacarbonyl mono-NBD complex **4**.²⁶ This was corroborated experimentally by heating a mixture of Co₂(CO)₈ and NBD under a CO atmosphere (1 bar). Under these conditions, the corresponding Co₂(CO)₆-NBD complex **4** was observed by in situ FT-IR spectroscopy as the major metal carbonyl complex in solution. Preparation of **4** and **5** has been described by reaction of Co₂(CO)₈ and NBD under nitrogen.²⁷ Under these conditions, the major isolated compound was Co₂(CO)₄-NBD₂ (**5**; lit. 2021 s, 1798 s cm⁻¹ in CCl₄/CS₂), while the mono-NBD complex **4** (lit. 2083 s, 2030 vs, 1820 s cm⁻¹ in CCl₄/CS₂) was isolated in low yield.

The cobalt carbonyl complex **4** formed at the end of the reaction was catalytically competent, as demonstrated in a consecutive PKR experiment (Figure 9). To this end, the pressure reactor was charged with TMSC₂H and NBD and 20 mol % of Co₂(CO)₈. The cyclization was performed as usual, and when the first batch of acetylene was consumed, a new fraction of TMSC₂H and NBD was added. This procedure allowed the reaction to restart up to four times, as observed in the ladder-like absorbance profile depicted in Figure 9. For the same experiment, in the metal carbonyl absorbance area, a switch between the alkyne complex **3** and the olefin intermediate **4** can be observed graphically (Figure 10).

The mixed order dependence with respect to catalyst concentration suggests that a dimerization pathway may occur to a certain degree in the reaction mechanism. Pauson and Khand described the formation of tetranuclear complex **6** and their corresponding η⁶-arene complexes in the stoichiometric PKR.²⁸ Tetracobalt dodecacarbonyl (**6**) is a catalyst for the PKR.^{13,29}

(25) PKR in heptane provided absorbances for the new intermediate at 2073, 2023, 2011, and 1833 cm⁻¹.

(26) Under the present reaction conditions, the dicobalt octacarbonyl complex was never observed by in situ FT-IR as an intermediate in the catalytic PKR.

(27) Winkhaus, G.; Wilkinson, G. *J. Chem. Soc.* **1961**, 602–605.

(28) Khand, I. U.; Knox, G. R.; Pauson, P. L.; Watts, W. E. *J. Chem. Soc., Perkin Trans. 1* **1973**, 975–977.

(29) Krafft, M. E.; Boñaga, V. R. *Angew. Chem., Int. Ed.* **2000**, *39*, 3676–3680.

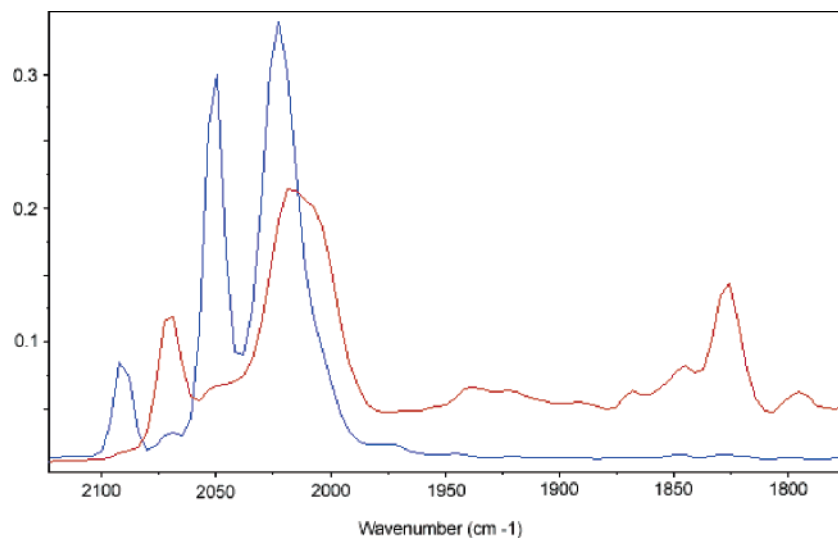


Figure 7. Metal carbonyl zone spectra during the catalytic PKR. The blue line corresponds to complex **3** (2092, 2050, and 2023 cm^{-1}) at the halfway point of conversion, and the red line corresponds to compound **4** (2069, 2019 (broad), and 1826 cm^{-1}) at the end of the reaction.

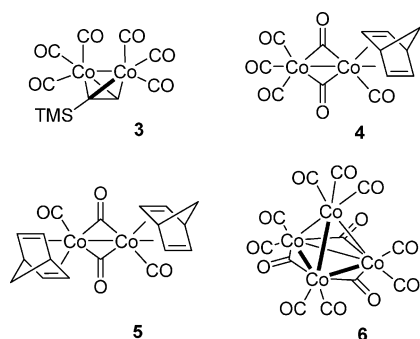


Figure 8.

However, there are no data available on the true catalytic species when $\text{Co}_4(\text{CO})_{12}$ is used as a metal source. To shed light on this matter, a catalytic PKR between TMSC_2H and NBD using **6** as a catalyst was set up and monitored by in situ FT-IR (Figure 11). Initial reaction spectra of the metal carbonyl area showed unreacted $\text{Co}_4(\text{CO})_{12}$ (**6**); however, at 77 °C under 2 bar of CO, the reaction rapidly evolved to provide the corresponding dicobalt alkyne complex **3** as a major metal carbonyl species in the reaction media. From this point, the catalytic PKR reaction evolved in a manner similar to that when $\text{Co}_2(\text{CO})_8$ was used as the metal source, and upon depletion of the alkyne substrate, the olefin complex **4** emerged as the final metal carbonyl product. As measured experimentally, TMSC_2H alone was responsible for the breakdown of the tetracobalt cluster into **3**. Reaction of **6** with the alkyne at 50 °C and 2 bar of CO provided full conversion to **3** within 45 min, as observed by FT-IR (Scheme 2). Under identical experimental conditions, reaction of **6** with NBD provided no conversion to the corresponding alkene complex **4**.³⁰

Kinetics and Mechanism for the Catalytic PKR. In 1985, Magnus proposed what is now the commonly accepted mechanism for the stoichiometric PKR.³¹ This mechanism describes the transformation of the alkyne hexacarbonyl complex **I** into the dicobalt cyclopentenone complex **V** (Scheme 3). Intensive

(30) Conversion of $\text{Co}_4(\text{CO})_{12}$ into **5** by reaction with NBD has been described; see: Kitamura, T.; Joh, T. *J. Organomet. Chem.* **1974**, *65*, 235–243.

(31) Magnus, P.; Exon, C.; Albaugh-Robertson, P. *Tetrahedron* **1985**, *41*, 5861–5869.

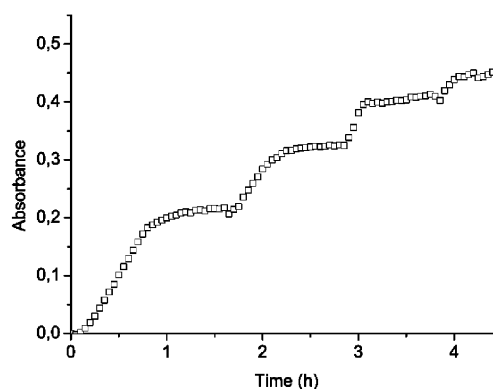


Figure 9. Reaction profile for a one-pot consecutive catalytic PKR. Reaction conditions: 80 °C, 2 bar of CO, 20 mol % initial catalyst loading.

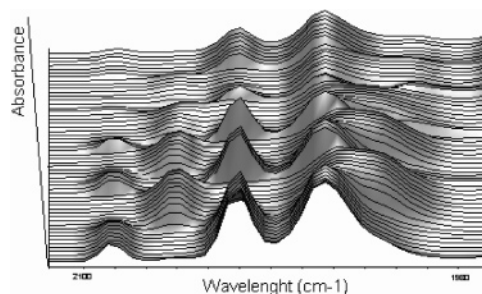


Figure 10. Terminal metal carbonyl zone (2100–1900 cm^{-1}) for the consecutive catalytic PKR experiment. A switch between complexes **3** and **4** is observed when the alkyne is depleted.

research effort has been devoted to validate the PKR mechanism by theoretical methods. Nakamura and Pericàs independently reported a complete DFT study for the transformation of **I** to **V**.³² Other authors have focused on the alkene coordination and alkene insertion steps to explain the regio- and stereoselectivity observed in the PKR.³³ For a catalytic cycle to conform to the Magnus mechanism, an alkyne–cyclopentenone exchange would suffice to regenerate **I** from **V** (Scheme 3). This represents the most straightforward manner to close a catalytic cycle for

(32) (a) Yamanaka, M.; Nakamura, E. *J. Am. Chem. Soc.* **2001**, *123*, 1703–1708. (b) Vázquez, J. Ph.D. Thesis, Universitat de Barcelona, 1999.

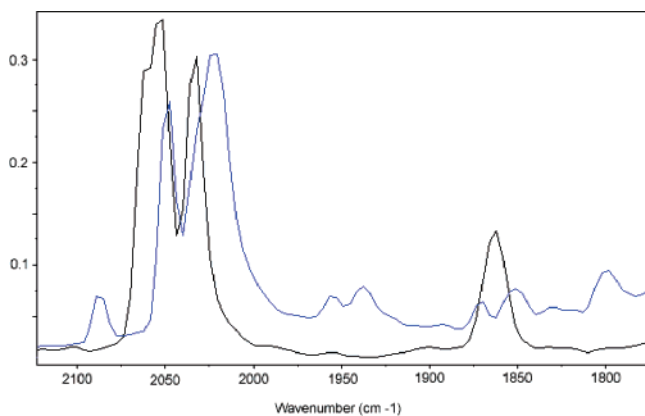
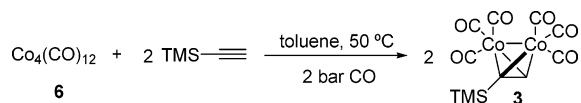


Figure 11. Metal carbonyl zone spectra during the catalytic PKR using $\text{Co}_4(\text{CO})_{12}$ as a catalyst. The initial reaction mixture spectrum (black line) shows absorbances of $\text{Co}_4(\text{CO})_{12}$ (2053 and 1860 cm^{-1}) and $\text{TMS-C}\equiv\text{C-H}$ (2034 cm^{-1}). After 1 h of reaction at $77\text{ }^\circ\text{C}$ (blue line), major carbonyl absorbances correspond to the alkyne complex **3** (2092 , 2050 , and 2023 cm^{-1}).

Scheme 2 . Breakdown of the Tetracobalt Dodecarbonyl Cluster with the Alkyne



the PKR. From the experimental point of view, however, little is known about the intermediate species involved in the PKR. To date, the corresponding dicobalt alkyne hexacarbonyl complex **I** is the only intermediate species that has been isolated and identified in the mechanism.³⁴

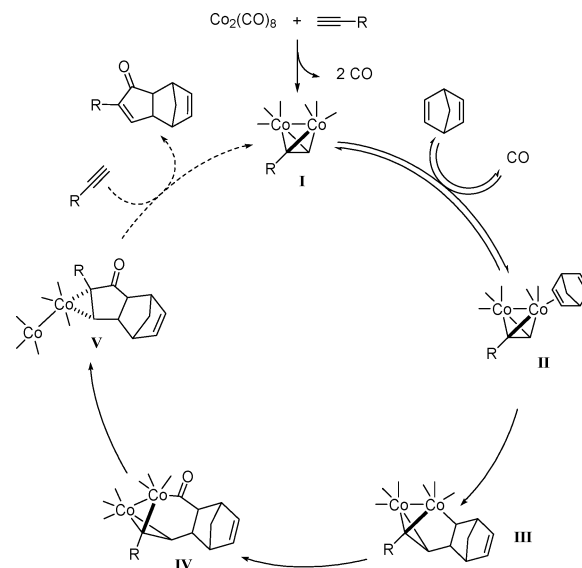
From our experimental data, the rate equation for the catalytic intermolecular PKR between $\text{TMS-C}\equiv\text{C-H}$ and NBD is

$$\nu = k[\text{Co}_2(\text{CO})_8]^{1.3}[\text{NBD}]^{0.3-1.2}[\text{CO}]^{-1.9}$$

Thus, the reaction rate is overall zero order with respect to alkyne concentration, 1.3 order with respect to catalyst concentration, between 0.3 and 1.2 order with respect to $[\text{NBD}]$, and -1.9 order with respect to $[\text{CO}]$. The observed rate equation suggests that a complex reaction mechanism is in operation in the catalytic intermolecular PKR of norbornadiene. Despite this complexity, a few conclusions may be drawn. The positive dependence on NBD and negative dependence on $[\text{CO}]$, along with the observation that the corresponding dicobalt alkyne complex **I** acts as a major resting state suggests that the CO –alkene ligand exchange is an energetically demanding equilibrium process preceding the rate-limiting step. Thus, the following alkene insertion to give **III** would be the rate-limiting step in the catalytic process. In this scenario, a higher concentration of NBD and lower concentration of $[\text{CO}]$ are beneficial for the kinetics of the reaction, since they favor formation of the key intermediate **II**.

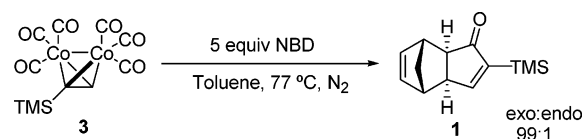
These experimental data are consistent with the overall catalytic cycle shown in Scheme 3 and the theoretical studies

Scheme 3 . Magnus Mechanism for the Stoichiometric PKR^a



^a CO ligands have been omitted for clarity.

Scheme 4 . Stoichiometric PKR of **3**



of Nakamura.³² However, the influence of the $[\text{CO}]$ pressure and NBD concentration on the stereoselectivity of the final PKR adducts is difficult to rationalize with this simple mechanism. We have shown that low $[\text{CO}]$ pressures and high NBD concentrations (*vide infra*) favor the formation of endo cyclization adducts (up to 14%). In contrast, the stoichiometric thermal reaction (N_2 , $77\text{ }^\circ\text{C}$) of **3** with NBD provided only 1% of the corresponding endo adduct (Scheme 4). The differential behavior between the stoichiometric and the catalytic reactions reveals that a second reaction pathway might be in operation in the catalytic reaction.

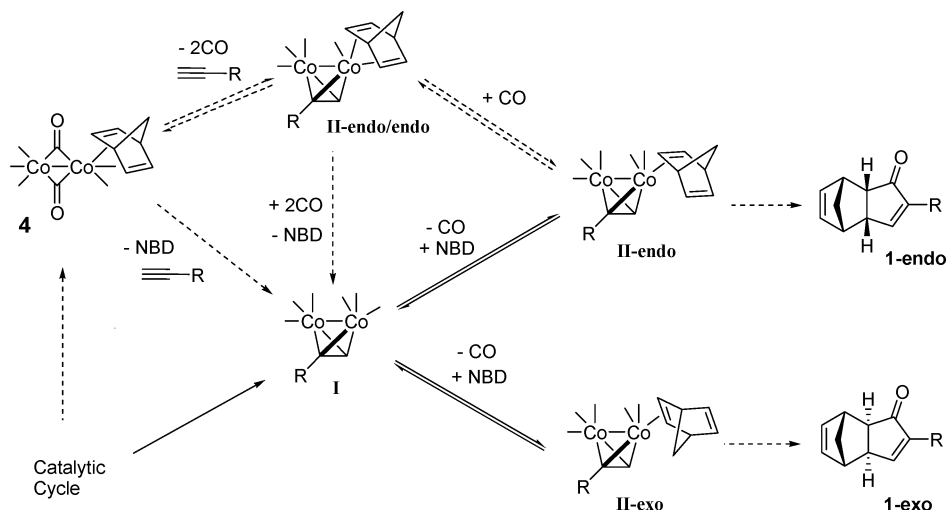
Exo and endo PKR adducts arise from stereoselective coordination of the double bond contained in NBD to the metal center. Thus, the complex **II-exo** will provide the adduct **1-exo**, while the complex **II-endo** is the origin of **1-endo** products (Scheme 5). Although **II-endo** is energetically less favored than the corresponding **II-exo** complex,³⁵ formation of **II-endo** from **I** through CO –alkene ligand exchange is expected to take place in the same proportion for both the catalytic and the stoichiometric reaction conditions. Thus, if we consider only equilibrium processes between complexes **I** and **II-exo/II-endo**, it is difficult to rationalize the difference in stereoselectivity for these two processes.

As we have shown in the consecutive PKR experiment, the NBD complex **4** is formed quantitatively in the absence of alkyne and is a catalytically viable intermediate in the regeneration of **3** (**I** in Scheme 5). Formation of **4** under $[\text{CO}]$ pressure discloses the tendency of NBD to act as a bidentate chelating ligand. Most interestingly, only double endo coordination allows NBD to work as a bidentate ligand. This double coordination of NBD will be facilitated under low $[\text{CO}]$ and high $[\text{NBD}]$.

(33) (a) Robert, F.; Milet, A.; Gimbert, Y.; Konya, D.; Greene, A. E. *J. Am. Chem. Soc.* **2001**, *123*, 5396–5400. (b) de Bruin, T. J. M.; Milet, A.; Robert, F.; Gimbert, Y.; Greene, A. E. *J. Am. Chem. Soc.* **2001**, *123*, 7184–7185. (c) de Bruin, T. J. M.; Milet, A.; Greene, A. E.; Gimbert, Y. *J. Org. Chem.* **2004**, *69*, 1075–1080.

(34) Dicobalt norbornene alkyne bis(diphenylphosphino)methane complexes have been detected by electrospray ionization mass spectroscopy; see: Gimbert, Y.; Lesage, D.; Milet, A.; Fournier, F.; Greene, A. E.; Tabet, J.-C. *Org. Lett.* **2003**, *5*, 4073–4075.

(35) Endo coordination of NBD is energetically disfavored by approximately 4.0 kcal/mol , as determined by DFT (B3LYP/LACVP) calculations.

Scheme 5. Feasible Ligand Exchange Processes in the Catalytic PKR of Norbornadiene^a

^a Metal carbonyl ligands have been omitted for clarity.

Table 3. Synthesis of Monophosphine Dicobalt Complexes

		$\text{Co}_2(\text{CO})_8\text{L}_2 \xrightarrow{\text{PR}_3} \text{Co}_2(\text{CO})_5\text{L}_2\text{PR}_3$			
entry no.	L ₂	PR ₃	conditions	yield (%)	product
1	2 CO	PPh ₃	THF, room temp	84	7
2	2 CO	P(OPh) ₃	THF, room temp	48	8
3	2 CO	P(OC ₆ H ₃ (Bu ^t) ₂) ₃	hexane, room temp	60	9
4	TMSC ₂ H	P(C ₆ H ₃ (CF ₃) ₂) ₃	toluene, 60 °C	70	10
5	TMSC ₂ H	PCy ₃	DME, 60 °C	22	11

These are exactly the conditions in which the highest ratio of the endo adduct is observed. Although no direct evidence confirms **4** as a catalytically significant intermediate, our experimental results suggest that involvement of **4** in the catalytic process might be the origin of the endo adduct. From **4**, reaction with the alkyne could provide **II-endo/endo**, which after CO uptake would yield **II-endo** (Scheme 5). Thus, within the catalytic cycle, formation of **4** could account for the formation of **II-endo** and ultimately the endo PKR adduct. This second reaction pathway is only possible for the catalytic process and could explain the difference in stereoselectivity between the stoichiometric and the catalytic reactions.

Finally, there is no direct evidence to explain the mixed order dependence with respect to $[\text{Co}_2(\text{CO})_8]$. As for most metal-catalyzed transformations, first-order kinetics with respect to catalyst concentration should be expected for the mechanism depicted in Scheme 4.²¹ A feasible explanation could be that a dimerization process occurs to a certain degree in the reaction. Cobalt carbonyl complexes are postulated to be involved in higher order bimolecular reaction mechanisms, as in the case of cobalt-catalyzed hydroformylation.³⁶ The $\text{Co}_2(\text{CO})_8$ complex dimerizes to afford the $\text{Co}_4(\text{CO})_{12}$ cluster (**6**) under thermal activation.³⁷ Another possibility is the breakup of the bimetallic catalyst into smaller fragments. In the presence of phosphine ligands $\text{Co}_2(\text{CO})_8$ suffers disproportionation into the ionic

species $[\text{Co}(\text{CO})_3\text{L}_2]^+$ and $[\text{Co}(\text{CO})_4]^-$.³⁸ This phenomenon is known to be reversible, and it may occur to a certain degree in the presence of NBD. Nevertheless, none of these species were observed by FT-IR analysis of the reaction mixtures. The intrinsic sensitivity threshold for this technique allows only detection of major catalytic species; minor catalytic components that may have a major kinetic effect could not be detected.

Dicobalt Phosphine Derivatives. Hexacarbonyl alkyne complexes and monophosphine complexes of $\text{Co}_2(\text{CO})_8$ have been described as catalyst substitutes in the PKR.^{39,40} Among these, phosphine complexes are of particular interest, since the phosphorus ligand remains attached to the metal complex throughout the catalysis. This is an interesting feature for the development of asymmetric versions of this process. In particular, dicobalt complexes modified with chiral diphosphines have been used successfully in the catalytic asymmetric intermolecular PKR.¹⁴ The most significant drawback for these systems is the lack of reactivity, which has been attributed to a decreased CO dissociation caused by the presence of phosphine ligands.⁴¹ In this context, we synthesized several dicobalt phosphine complexes and studied how the electronic and steric effects of the phosphine moiety influence the catalytic intermolecular PKR.

The synthesis of dicobalt monophosphine complexes is described in Table 3. $\text{Co}_2(\text{CO})_7\text{PR}_3$ complexes **7–9** were prepared by following small variations of procedures described in the literature, which gave good to excellent yields (Table 3, entries 1–3).³⁹ In contrast, direct reaction of $\text{Co}_2(\text{CO})_8$ with $\text{P}(\text{C}_6\text{H}_3(\text{CF}_3)_2)_3$ and PCy_3 led to decomposition of the dicobalt complex. In these two cases, the corresponding dicobalt pentacarbonyl TMSC_2H complexes **10** and **11** were synthesized as dicobalt monophosphine surrogates (Table 3, entries 4 and 5). With the phosphine complexes in hand, their efficiency in the catalytic PKR was examined at 80 °C and 2 bar of CO (Figure 12). On the basis of the reaction profiles in Figure 12,

(38) Szabo, P.; Fekete, L.; Bor, G.; Nagy-Magos, Z.; Marko, L. *J. Organomet. Chem.* **1968**, *12*, 245–248.

(39) (a) Comely, A. C.; Gibson, S. E.; Stevenazzi, A.; Hales, N. J. *Tetrahedron Lett.* **2001**, *42*, 1183–1185. (b) Gibson, S. E.; Johnstone, C.; Stevenazzi, A. *Tetrahedron* **2002**, *58*, 4937–4942.

(40) Belanger, D. B.; Livinghouse, T. *Tetrahedron Lett.* **1998**, *39*, 7641–7644.

(41) van Leuven, P. W. N. *Homogeneous Catalysis*; Kluwer Academic: Dordrecht, The Netherlands, 2004.

(36) For examples of bimetallic hydroformylation mechanisms see: (a) van Boven, M.; Alemdaroglu, N. H.; Penninger, J. M. L. *Ind. Eng. Chem. Prod. Res. Dev.* **1975**, *14*, 259–264. (b) Azran, J.; Orchin, M. *Organometallics* **1984**, *3*, 197–199. (c) Li, C.; Widjaja, E.; Garland, M. *J. Am. Chem. Soc.* **2003**, *125*, 5540–5548.

(37) (a) Ungvary, F.; Marko, L. *Inorg. Chim. Acta* **1970**, *4*, 324–326. (b) Ungvary, F.; Marko, L. *J. Organomet. Chem.* **1974**, *71*, 283–286.

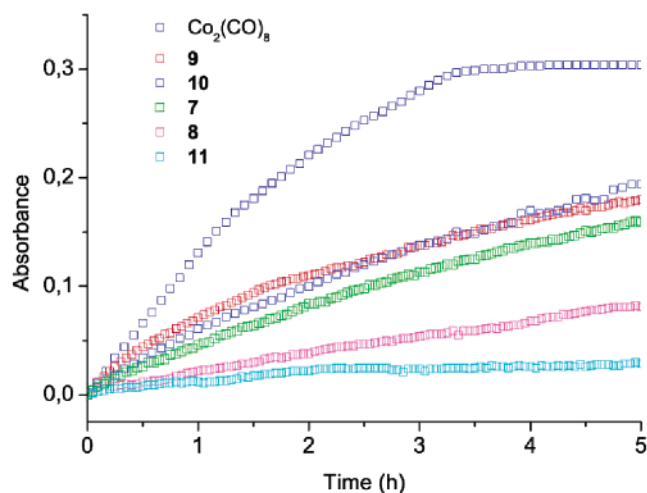


Figure 12. Reaction profile using a range of cobalt catalysts. Reaction conditions: [cat] = 11.9 mM, [TMSC₂H]₀ = 0.41 M, [NBD]₀ = 0.82 M, 80 °C, 2 bar of CO.

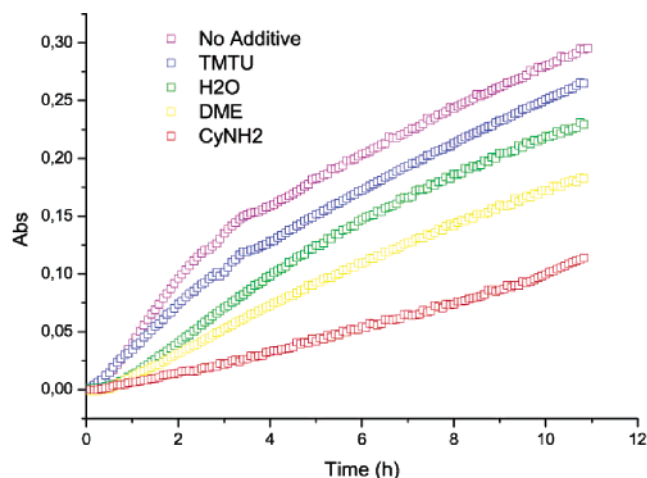


Figure 13. Reaction profile upon addition of distinct Lewis base additives. Reaction conditions: 70 °C, [Co₂(CO)₈] = 11.9 mM, [TMSC₂H]₀ = 0.41 M, [NBD]₀ = 0.82 M, 0.5 bar of CO.

we can draw a major conclusion: the introduction of a phosphine ligand on Co₂(CO)₈ has a deleterious effect on the reaction rate with respect to the parent system. Among the phosphine complexes studied, electron-rich PCy₃ presented the lowest reaction rate, while electron-deficient P(C₆H₃(CF₃)₂)₃ provided the fastest rate. The electronic effects observed are in agreement with the notion that CO dissociation is an energetically demanding step in the catalytic cycle. Electron-rich phosphines hamper CO dissociation because of metal–CO back-bonding, while electron-deficient phosphines show the opposite behavior.⁴¹

Other Lewis Base Additives. Nucleophilic substances have been used as additives in either the stoichiometric or the catalytic PKR. It has been postulated that Lewis base additives facilitate the dissociative step, in which a carbonyl ligand is replaced by the incoming olefin. Among the additives used for this purpose, perhaps the most widely studied are cyclohexylamine, water, and dimethoxyethane.^{9,10} Tetramethylthiourea (TMTU) has recently been used as a promoter for the catalytic intramolecular PKR.⁸ In some instances, the use of additives are claimed to allow the catalytic PKR to run at atmospheric CO pressure.⁸ To see whether these substances have truly a positive rate enhancement in the catalytic intermolecular PKR, we tested several additives and monitored the reaction by FT-IR. Reactions

Table 4. Product Distribution for Catalytic PKR Performed in the Presence of Additives

additive	1-exo (%)	1-endo (%)	2a (%)	2b (%)	exo:endo
TMTU	88.2	6.3	3.8	1.7	14:1
H ₂ O	92.3	2.3	4.0	1.4	40:1
DME	89.3	6.3	3.2	1.2	14:1
CyNH ₂	88.7	7.0	3.3	1.0	13:1
	90.8	6.0	2.3	0.9	15:1

were performed at 70 °C and 3 mol % of Co₂(CO)₈ in toluene and 0.5 bar of CO overpressure.⁴² Reaction profiles when using TMTU (18 mol %), water (17 mol %), DME (12 mol %), and CyNH₂ (18 mol %) were compared with a reaction with no additives (Figure 13). Recorded data are shown up to 11 h, which is the time the reaction lacking any additive takes to reach completion. From this graphic, we can conclude that the addition of Lewis base additive had a deleterious effect on the reaction rate (Figure 13). Thus, cyclohexylamine produced the largest adverse effect on the reaction rate, while TMTU provided only a slight decrease with respect to Co₂(CO)₈ alone. Product selectivity for reactions in the presence of additives provides further data for analysis (Table 4). Reactions using water, DME, or CyNH₂ provided a product distribution similar to that of dicobalt octacarbonyl alone. However, TMTU afforded higher exo/endo selectivity, up to 40:1. This observation indicates that, under these experimental conditions, TMTU may effectively bind to the catalyst while other additives produce only catalyst decomposition. Thus, we can conclude that Lewis base additives do not produce an effective rate increase in the intermolecular PKR of NBD. However, their presence may either enhance product selectivity or improve product isolation.

Conclusion

Reaction progress analysis performed by in situ FT-IR has allowed the study of the kinetics of a cobalt-catalyzed intermolecular PKR for the first time. Thus, rate dependences with respect to the individual substrates were calculated, and we observed that the reaction was –1.9 order with respect to CO pressure, zero order with respect to TMSC₂H, between 0.3 and 1.2 order with respect to NBD, and 1.3 order with respect to Co₂(CO)₈. IR analysis of the metal carbonyl intermediates in a consecutive catalytic PKR experiment revealed two major reaction intermediates: the corresponding dicobalt hexacarbonyl alkyne complex **3**, which is the major catalyst resting state, and the dicobalt hexacarbonyl NBD complex **4**, which can be observed in the absence of the alkyne. These experimental observations suggest that the corresponding alkene insertion is the rate-limiting step in the catalytic process studied here. A detailed ligand exchange process between the dicobalt carbonyl species is proposed to account for the difference in stereoselectivity between the stoichiometric and the catalytic process. The use of Co₄(CO)₁₂ as a catalyst source in the PKR by FT-IR was also studied, and we have shown that upon reaction with TMSC₂H both Co₂(CO)₈ and Co₄(CO)₁₂ provide identical intermediate profiles. We also examined the use of phosphine-modified catalysts and the addition of Lewis bases. Both strategies had a deleterious effect on the reaction kinetics with respect to the use of dicobalt octacarbonyl alone.

Experimental Section

Reagents and Methods. Solvents were distilled from appropriate reagents prior to use. Co₂(CO)₈ stabilized with hexane (10 wt %)

(42) A low overpressure of CO was selected to mimic reactions at atmospheric pressure (balloon pressure).

was purchased from Fluka and used without further purification. All reactions were conducted under a nitrogen or argon atmosphere using standard Schlenk techniques. Silica gel used for filtration and flash chromatography of cobalt complexes was previously washed with Et₂O. In some dicobalt alkyne complexes, due to a deficient relaxation of the carbon cluster atoms, the corresponding signals were not observed in the ¹³C NMR spectra. Medium pressure reaction kinetic measurements were recorded on a ReactIR 4000 from Mettler-Toledo with an immersible ATR SiComp probe fitted onto a 50 mL Miniclave glass reactor from Buchi AG. Dicobalt heptacarbonyl complexes **7** and **8** were synthesized by following reported experimental procedures.⁴⁰

Dicobalt Heptacarbonyl Complex of Tris(2,4-di-*tert*-butylphenyl)phosphate (9). A Schlenk tube was charged with dicobalt octacarbonyl (490 mg, 1.29 mmol). A solution of tris(2,4-di-*tert*-butylphenyl) phosphite (701 mg, 1.06 mmol) in hexane (12 mL) was added to this solid. The system was purged with argon, and the reaction mixture was stirred at room temperature overnight, which resulted in a brown precipitate. The solid was filtered and washed with cold hexane. The solid was dried under vacuum to afford 633 mg (60%) of **9** as a brown powder. IR (KBr): ν_{\max} 1982 vs, 2003 s, 2058 w cm⁻¹. ¹H NMR (400 MHz, C₆D₆): δ 1.10 (s, 27H), 1.60 (s, 27H), 6.95 (s, 3H), 7.50 (s, 3H), 7.33 (d, $J = 7$ Hz, 3H) ppm. ¹³C NMR (75 MHz, CDCl₃): δ 30.7 (s, CH₃), 31.4 (s, CH₃), 34.5 (s, Cq), 35.4 (s, Cq), 120.0 (s, *o*-Ar CH), 124.3 (s, *m*-Ar CH), 125.1 (s, *p*-Ar CH), 139.0 (s, *o*-Ar Cq), 147.1 (s, *p*-Ar Cq), 148.9 (s, Cq-O), 201.8 (br s, Co(CO)). ³¹P NMR (121 MHz, CDCl₃): δ 155.8 (s, 1P) ppm.

Dicobalt Pentacarbonyl Complex of (Trimethylsilyl)acetylene and Tris(3,5-bis(trifluoromethyl)phenyl)phosphine (10). A Schlenk tube was charged with toluene (1 mL) and the dicobalt hexacarbonyl complex of Me₃SiCCH (86 mg, 0.22 mmol). A solution of tris-(3,5-bis(trifluoromethyl)phenyl)phosphine (107 mg, 0.15 mmol) in toluene (4 mL) was added to this mixture. The system was purged with argon, and the reaction mixture was heated to 60 °C. After 4 h, the resulting mixture was purified by flash chromatography (SiO₂/hexane) to yield 119 mg (70%) of **10** as a red oil that solidifies upon standing. IR (film): ν_{\max} 2012 vs, 2071 vs cm⁻¹. ¹H NMR (400 MHz, CDCl₃): δ 0.18 (s, 9H), 5.58 (d, $J_P = 8$ Hz, 1H), 7.86 (d, $J = 10$ Hz, *o*-Ar H, 6H), 8.06 (s, *p*-Ar H, 3H) ppm. ¹³C NMR (100 MHz, C₆D₆): δ 0.7 (s, CH₃), 80.8 (d, $J_P = 6$ Hz, Cq), 87.0 (d, $J_P = 4$ Hz, CH), 122.9 (d, $J_F = 272$ Hz, CF₃), 125.3 (s, *p*-Ar CH), 132.6 (d, $J_P = 10$ Hz, *m*-Ar CH), 133.2 (dd, $J_P = 9$ Hz, $J_F = 34$ Hz, *m*-Ar C), 137.4 (d, $J_P = 34$ Hz, ipso-Ar C) ppm. ¹⁹F NMR (376 MHz, CDCl₃): δ 63.6 (s) ppm. ³¹P NMR (121 MHz, C₆D₆):

δ 57.01 (s) ppm. MS (FAB⁺): m/z 1026 (M⁺, 5%), 970 ([M - 2CO]⁺, 50%), 914 ([M - 4CO]⁺, 100%).

Dicobalt Pentacarbonyl Complex of (Trimethylsilyl)acetylene and Tricyclohexylphosphine (11). A Schlenk tube was charged with DME (2 mL) and the dicobalt hexacarbonyl complex of Me₃-SiCCH (440 mg, 1.15 mmol). A solution of tricyclohexylphosphine (204 mg, 0.73 mmol) in DME (4 mL) was added to this mixture. The system was purged with argon, and the reaction mixture was heated to 60 °C. After 4 h, the resulting mixture was purified by flash chromatography (SiO₂/hexane) to yield 101 mg (22%) of **11** as a red oil that solidifies upon standing. IR (KBr): ν_{\max} 1950 s, 1972 s, 1991 vs, 2049 vs cm⁻¹. ¹H NMR (400 MHz, CDCl₃): δ 0.27 (s, 9H), 1.26–1.96 (m, 33H), 5.81 (d, $J_P = 4$ Hz, 1H) ppm. ¹³C NMR (100 MHz, C₆D₆): δ 2.5 (s, CH₃), 26.6 (s, CH₂), 27.7 (d, $J_P = 9$ Hz, CH₂), 27.8 (d, $J_P = 9$ Hz, CH₂), 29.7 (d, $J_P = 12$ Hz, CH₂), 37.6 (d, $J_P = 16$ Hz, CH), 70.6 (s, Cq), 82.7 (s, CH), 203.2, 208.5, 209.7 (br s, CO) ppm. ³¹P NMR (121 MHz, C₆D₆): δ 63.0 (s) ppm. MS (FAB⁺): m/z 636 (M⁺, 6%), 608 ([M - CO]⁺, 65%).

Pauson–Khand Reaction Monitored by IR Spectroscopy. In a typical experiment, the glass reactor was charged in this order: with toluene (15 mL), (trimethylsilyl)acetylene (1.4 mL, 9.6 mmol), norbornadiene (2.0 mL, 19.2 mmol), and Co₂(CO)₈ (109 mg, 0.287 mmol). Extra toluene (5 mL) was used to wash out the catalyst from the addition funnel. The reactor was immediately sealed, purged with CO, charged to the designated CO pressure, and immersed in a water bath at the appropriate temperature. At this point, the spectrometer was set to collect one spectrum every 5 min. Profiles at 1698 cm⁻¹ were collected after baseline correction and analyzed.

Acknowledgment. This work was supported by the MEC (No. CTQ2005-00623). X.V. thanks the DURSI for “Distinció per a la Promoció de la Recerca Universitària”. Rafel Prohens and the “Plataforma de Química Fina” are kindly acknowledged for support in FT-IR technology. We thank Prof. A. Moyano and Prof. P. Cabot for insightful comments on the manuscript.

Supporting Information Available: Graphical representations of the reaction rate vs alkyne concentration (Figure 1-S) and reaction profile dependence on alkyne concentration (Figure 2-S) and IR and ¹H and ¹³C NMR spectra for compounds **9–11**. This material is available free of charge via the Internet at <http://pubs.acs.org>.

OM060935+